Materials Research Bulletin 84 (2016) 65–70

Contents lists available at ScienceDirect

Materials Research Bulletin

journal homepage: www.elsevier.com/locate/matresbu

Z-scheme TiO_2/g-C_3N_4 composites with improved solar-driven photocatalytic performance deriving from remarkably efficient separation of photo-generated charge pairs

Shengtian Huang[a], Junbo Zhong[a,*], Jianzhang Li[a,*], Jiufu Chen[a], Zhen Xiang[a], Wei Hu[a], Minjiao Li[a,b]

[a] Key Laboratory of Green Catalysis of Higher Education Institutes of Sichuan, College of Chemistry and Environmental Engineering, Sichuan University of Science and Engineering, Zigong, 643000, PR China
[b] Sichuan Provincial Academician (Expert) Workstation, Sichuan University of Science and Engineering, Zigong, 643000, PR China

ARTICLE INFO

Article history:
Received 13 June 2016
Received in revised form 20 July 2016
Accepted 31 July 2016
Available online 1 August 2016

Keywords:
A. semiconductors
A. inorganic compounds
A. interfaces
B. chemical synthesis
D. catalytic properties

ABSTRACT

High recombination rate of electron-hole pairs and weak oxidation ability of holes from g-C_3N_4 greatly limit the catalytic degradation efficiency of g-C_3N_4-based photocatalysts, thus it is crucial to further improve the photocatalytic efficiency of g-C_3N_4. In this paper, TiO_2 was successfully loaded onto the g-C_3N_4 surface to induce the electron–hole separation and enhance the photocatalytic efficiency. The results revealed the maximum photocatalytic performance toward discoloration of methyl orange (MO) aqueous solution under the simulated sunlight illumination at molar ratio of 3% TiO_2 to g-C_3N_4 composite. The junction between TiO_2 and g-C_3N_4 significantly accelerate the separation of the photo-generated charge pairs caused by the strong interactions between TiO_2 and g-C_3N_4. Such highly efficient photo-generated charge separation can be explained by a Z-scheme charge separation and migration mechanism based on the results of the scavenger experiments and the energy band structures.

1. Introduction

As a metal-free and narrow bandgap semiconductor, graphitic carbon nitride (g-C_3N_4) has triggered great interests since its photocatalytic properties were reported by Wang in 2009 [1]. More importantly, g-C_3N_4 displays prominent thermal stability, reliable chemical inertness, non-toxicity, easy modification, and excellent electrical property [1–3], which making g-C_3N_4 one of the most attractive photocatalysts for the future application. Due to its unique features, the photocatalytic performance of g-C_3N_4 has been extensively studied, however, the photocatalytic properties of g-C_3N_4 is greatly hindered by its inherent drawbacks, such as the high recombination rate of photo-generated electrons and holes, lower specific surface area, and low quantum efficiency [4–6]. Moreover, the relative low valence band (VB) edge potential (−1.4 eV vs. NHE) of g-C_3N_4 limits the photo-induced hole from g-C_3N_4 from oxidizing into H_2O or OH^- in order to generate ·OH, which further decreases the photocatalytic performance of g-C_3N_4. Consequently, it is essential to promote the separation of photo-generated charge pairs and generate more ·OH to improve the photocatalytic performance of g-C_3N_4 based photocatalysts. To solve this issue, tremendous efforts have been put into improving the photocatalytic performance of g-C_3N_4 by doping [7,8], fabricating novel structures [9,10], coupling g-C_3N_4 with graphene [11,12] and so on.

Among all these strategies, construction of heterostructures is an effective method to enhance the photocatalytic activity, which can significantly promote the separation of photo-generated charge pairs due to the different energy band structures of photocatalysts, resulting in high separation efficiency of photo-generated charge pairs. To achieve this goal, the photocatalysts must have matched energy band potentials. Compare to the normal hydrogen electrode (NHE), the conduction band (CB) and the VB of g-C_3N_4 is −1.3 eV and 1.4 eV at pH 7.0, respectively [13]. It is evident that the electron from the CB of g-C_3N_4 has strong reduction ability, while the hole from the VB of g-C_3N_4 exhibits weak oxidation ability. To maintain the strong reduction ability of the electron from the CB of g-C_3N_4 and offset the weak oxidation ability of the hole from the VB of g-C_3N_4, the counterpart should have suitable energy band potentials, and the separation of the

---

* Corresponding authors.

E-mail addresses: sth499@163.com (S. Huang), junbozhong@163.com (J. Zhong), lyl63@sina.com (J. Li), 876387500@qq.com (J. Chen), lschmanuscript@163.com (Z. Xiang), huwei2113061@163.com (W. Hu), lmj0621@126.com (M. Li).

http://dx.doi.org/10.1016/j.materresbull.2016.07.036
0025-5408/© 2016 Elsevier Ltd. All rights reserved.

charge pairs should have another routine which is different from the common one, otherwise the heterostructures should sacrifice the strong reduction ability of the electron from the CB of g-C_3N_4. Thus, seeking a semiconductor with matched energy band potentials is a challenging task. Among the photocatalysts used to couple with g-C_3N_4, TiO_2 is thought to be an ideal candidate due to the CB and VB edge potential of TiO_2 are more positive than that of g-C_3N_4. The photo-generated charge separation can be greatly promoted owing to the interfacial electric field when TiO_2 is coupled with g-C_3N_4. Meanwhile, the photo-induced CB electrons from TiO_2 can transfer to the VB of g-C_3N_4, resulting in the recombination of electrons and holes. Therefore, the VB holes with strong oxidation ability can be accumulated on TiO_2 and CB electrons with strong reduction ability are accumulated on g-C_3N_4, increasing the separation efficiency of photo-induced charge pairs and oxidation/reduction of the electrons and hole. To test this assumption, TiO_2/g-C_3N_4 composite photocatalysts have been fabricated, and the corresponding photocatalytic activities were evaluated by many groups, the results revealed that coupling TiO_2 with g-C_3N_4 can promote the photocatalytic performance of bare TiO_2 and g-C_3N_4 [14–20]. Based on the observations, charge separation mechanism was proposed. However, it is worth noting that there are a few scattered and contradictory results of charge separation mechanism from the literatures. Furthermore, the photo-induced charge separation behavior (rate and phase) of TiO_2/g-C_3N_4 and the relation of charge separation behavior with the photocatalytic performance of composites remain unclear, and needs to be further studied. In fact, the information on the photo-induced charge separation behavior (charge separation rate and phase) can provide critical information on the charge separation mechanism and the nature of the photocatalytic reaction.

Herein, the photo-induced charge separation and migration behavior of TiO_2/g-C_3N_4 photocatalysts was investigated using SPV, and the corresponding photocatalytic activities of heterostructures were evaluated by the discoloration of MO aqueous solution under a simulated sunlight irradiation. Based on the results, a Z-scheme charge separation and migration mechanism was proposed to explain the enhancement of the solar-driven photocatalytic performance deviating from the promoted photo-generated charge separation properties.

2. Experimental section

2.1. Preparation of catalysts

All chemicals were of analytical purity and used as received. Deionized water was employed in photocatalytic experiments. g-C_3N_4 was prepared as the procedure described in Ref. [21] by heating urea. TiO_2 sol was prepared by a sol-gel routine according to the procedure given in Ref. [22] using tetrabutylorthotitanate, diethanolamine and ethanol as the raw materials.

TiO_2/g-C_3N_4 composite photocatalysts with different molar ratios of TiO_2 and g-C_3N_4 were prepared by a pore impregnating method using calcinating TiO_2 sol at 723 K for 2 h. The samples with different molar ratios of TiO_2 and g-C_3N_4 (1%, 2%, 3% and 4%, respectively) were marked as 1%, 2%, 3% and 4%, respectively. TiO_2 was prepared by baking the TiO_2 gel at 723 K for 2 h. g-C_3N_4 was also treated as the method mentioned above without the presence of tetrabutylorthotitanate and named as 0%.

Table 1
Specific surface area of photocatalysts.

Catalysts	0%	1%	2%	3%	4%
S_{BET} (m^2/g)	20	25	26	29	28

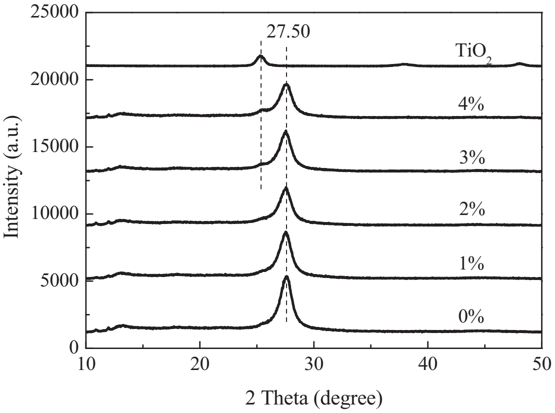

Fig. 1. XRD patterns of photocatalyst.

2.2. Characterization of samples

Specific surface area was measured on a SSA-4200 automatic surface analyzer by N_2 adsorption method at 77 K. The crystal phases of the photocatalysts were analyzed by a DX-2600 X-ray diffractometer. The morphology of photocatalysts was observed on a JSM-7500F scanning electron microscopy (SEM). The UV–Vis DRS in the wavelength range between 230 and 800 nm was conducted on a UV–Vis spectrophotometer (TU-1907). XPS spectra were performed on an XSAM 800 using Mg Kα at 12 kV and 12 mA. The X-ray photoelectron spectra were referenced to the C1 s peak (*BE* = 284.80 eV). To study the separation properties of the photo-

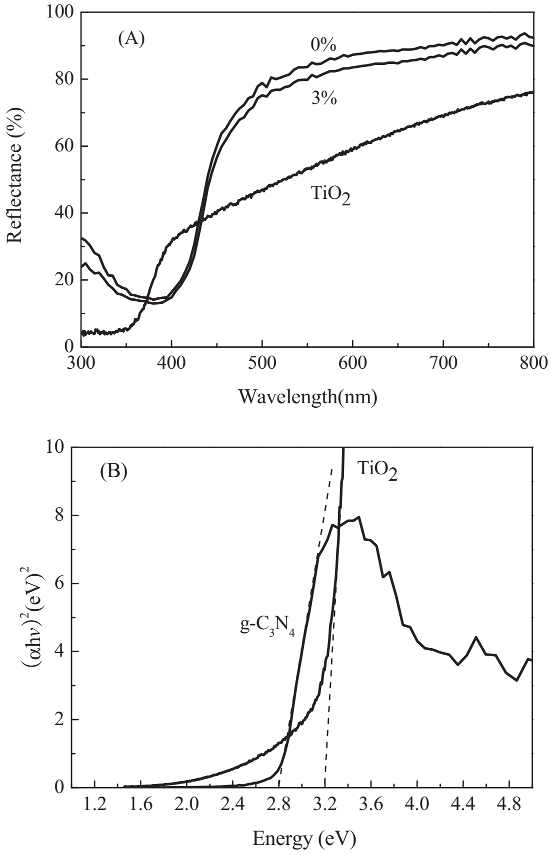

Fig. 2. (a) UV–Vis DRS of photocatalysts; (b) relationship between $(\alpha h\nu)^2$ and energy.